Journal of Systems Engineering and Electronics
Vol. 32, No. 3, June 2021, pp.527 – 537

Direction of arrival estimation method based on quantum electromagnetic field optimization in the impulse noise

DU Yanan, GAO Hongyuan*, and CHEN Menghan

College of Information and Communication Engineering, Harbin Engineering University, Harbin 150001, China

Abstract: In order to resolve direction finding problems in the impulse noise, a direction of arrival (DOA) estimation method is proposed. The proposed DOA estimation method can restrain the impulse noise by using infinite norm exponential kernel covariance matrix and obtain excellent performance via the maximum-likelihood (ML) algorithm. In order to obtain the global optimal solutions of this method, a quantum electromagnetic field optimization (QEFO) algorithm is designed. In view of the QEFO algorithm, the proposed method can resolve the difficulties of DOA estimation in the impulse noise. Comparing with some traditional DOA estimation methods, the proposed DOA estimation method shows high superiority and robustness for determining the DOA of independent and coherent sources, which has been verified via the Monte-Carlo experiments of different schemes, especially in the case of snapshot deficiency, low generalized signal to noise ratio (GSNR) and strong impulse noise. Beyond that, the Cramér-Rao bound (CRB) of angle estimation in the impulse noise and the proof of the convergence of the QEFO algorithm are provided in this paper.

Keywords: direction of arrival (DOA) estimation, impulse noise, infinite norm exponential kernel covariance matrix, maximum-likelihood (ML) algorithm, quantum electromagnetic field optimization (QEFO) algorithm, Cramér-Rao bound (CRB).

DOI: 10.23919/JSEE.2021.000044

1. Introduction

Direction of arrival (DOA) estimation is usually called spatial spectrum estimation or direction finding. It has been widely used in mobile communication and satellite communication systems, information warfare, radar, passive sonar, seismology, radio frequency astronomy, navigation, sound source tracking, microphone array, spectrum estimation and so on [1−3]. Schmidt et al. [4] proposed the multiple signal classification (MUSIC) algorithm in 1986, which pioneered the subspace-based array signal processing algorithm and realized high-resolution direction finding of arrays in a real sense [5]. The MUSIC method is universally accepted as an efficient and asymptotically unbiased estimation method for targets locating in the Gaussian noise [6,7].

Over several decades, several subspace-based DOA estimation algorithms have received considerable attentions. A maximum-likelihood (ML) method of stochastic sources which may be correlated was presented in [8]. A noise subspace fitting (NSF) algorithm was proposed by using the noise subspace fitting criterion function in [9]. Han et al. [10] proposed an estimation method of signal parameters via rotational invariance techniques (ESPRIT) algorithm, which uses the rotation invariant feature of signal subspace to locate targets, avoids the large amount of computation produced by the MUSIC algorithm in the whole search domain due to search at quantization interval, and reduces the hardware requirements of the algorithm to some extent, but the performance of the ESPRIT algorithm is inferior to that of the MUSIC algorithm [11,12].

Most of the classical DOA estimation methods are only applicable to Gaussian noise. However, non-Gaussian noise with impulse characteristics, such as atmospheric noise (thunderstorms), underwater noise, low-frequency atmospheric noise and some artificial noise are considered in the practical application environment and all of them can be described by symmetric α-stable (SαS) distribution with different characteristic exponent α [13,14]. The second-order and higher-order moment methods applied to the Gaussian model cannot be applied to non-Gaussian SαS distribution because impulse noise does not have second-order and higher-order moments. Hence, taking impulse noise as the research object of DOA estimation and designing a more generalized DOA estimation method to improve the robustness of the DOA estimation method in the impulse noise will greatly expand the

Manuscript received June 01, 2020.
*Corresponding author.
This work was supported by the National Natural Science Foundation of China (61571149), the Natural Science Foundation of Heilongjiang Province (LH2020F017), the Initiation Fund for Postdoctoral Research in Heilongjiang Province (LBH-Q19098), and the Heilongjiang Province Key Laboratory of High Accuracy Satellite Navigation and Marine Application Laboratory (HKL-2020-Y01).

application scope of existing DOA estimation methods.

It is generally known that the traditional DOA estimation methods on account of second and higher-order moments will lose effectiveness in the impulse noise. With respect to this problem, the robust covariation (ROC) was used for inhibiting the impulse noise, and the ROC-MUSIC method was put forward for DOA estimation in [15]. However, it requires large sample sizes for a satisfactory performance. The fractional lower order moment MUSIC (FLOM-MUSIC) DOA estimation method was presented in [16]. However, the performance of FLOM-MUSIC deteriorates seriously in the strong impulse noise $0<\alpha<1$ which is limited in the range of $1<\alpha<2$. You et al. [17] proposed a FLOC-MUSIC method using the fractional lower order cyclic covariance (FLOC) matrix. However, the FLOM-MUSIC method and FLOC-MUSIC need prior information of the characteristic index α, in order to avoid estimating the noise characteristic index, an infinity-norm normalization MUSIC (IN-MUSIC) algorithm for received data was put forward in [18]. Although the ML algorithm [19] has a more accurate estimation result compared with these subspace-based algorithms, the performance of the ML algorithm deteriorates seriously in the background of impulse noise. Zhao et al. [20] proposed a FLOC-ML DOA estimation method on account of FLOM matrices, but the performance deteriorates seriously in the strong impulse noise $0<\alpha<1$. The correntropy has been proposed by applying a translation-invariant kernel which can obtain more information than the traditional correlation functions [21,22]. In order to restrain the strong impulse noise and obtain more information, we are the first to introduce the exponential kernel (EK) covariance matrix to the ML method and propose the infinite norm exponential kernel maximum likelihood (INEK-ML) method for DOA estimation.

The INEK-ML method is difficult to be put into effect because the optimization objective for the INEK-ML method is high-dimensional, nonlinear, and multimodal, which needs the maximization of the cost function. In this context, intelligent optimization algorithms have been greatly developed. They have an excellent performance when optimizing the objective function of the INEK-ML DOA estimation method in terms of reducing the runtime and improving the speed of convergence.

At present, some scholars have researched on intelligence optimization algorithms in detail, for example, particle swarm optimization (PSO) [23], genetic algorithm (GA) [24], artificial bee colony (ABC) [25], and glowworm swarm optimization (GSO) [26] have got significant progress in various domains [27,28] because of their simplicity and derivation-free mechanism. However, there is a contradiction between convergence speed and convergence accuracy for these traditional intelligence optimization algorithms in solving complex optimization problems, a larger population size and more iterations are required when solving high-dimensional optimization problems, which increases the computational cost, especially in the DOA estimation problem. Hence, on account of quantum computing [29] and the principle of the electromagnetic field in physics [30], a quantum electromagnetic field optimization (QEFO) algorithm has been put forward in this paper. The proposed QEFO algorithm can eliminate the contradiction between convergence speed and convergence accuracy and improve the global search ability compared with the electromagnetic field optimization (EFO) [30]. Therefore, QEFO can be applied to solve the objection function of INEK-ML, which is denoted as the QEFO-INEK-ML method for short.

In order to analyze the performance of the QEFO-INEK-ML method, we prove that the QEFO algorithm is convergent, and present a universal representation of the Cramér-Rao bound (CRB) for DOA estimation in the impulse noise. Then, the performance of the QEFO-INEK-ML method has been verified through different DOA estimation scenarios, including the number of snapshots, sources, antennas, and the characteristic exponent. The desired performance in different DOA estimation scenarios can be received by the proposed QEFO-INEK-ML method through the simulation results of Monte Carlo experiments.

In summary, the important contributions of this paper are summarized as below:

(i) The DOA estimation method can restrain the impulse noise without estimating the characteristic index of noise, and obtain the expected performance for DOA estimation with snapshot deficiency and a low generalized signal noise to ratio (GSNR).

(ii) There are no need for additional pretreatment techniques for the proposed DOA estimation method to locate coherent sources.

(iii) An intelligence optimization algorithm called QEFO is proposed, and QEFO can be applied to resolve the optimal solution of the INEK-ML method.

(iv) The convergence of the QEFO algorithm is proved by the mathematical analysis.

(v) A universal representation of the CRB for DOA estimation in the impulse noise is presented by mathematical derivation.

The rest of this paper is arranged as below: In Section 2, the DOA estimation model in the impulse noise and the INEK-ML method are researched. In Section 3, the QEFO algorithm is represented fully and the convergence of QEFO is analyzed, after that, QEFO is used for resolving the cost function of the INEK-ML method. In

Section 4, the CRB which can be used for analyzing the performance of the proposed DOA estimation method is derived in the background of impulse noise. In Section 5, the superiority of the proposed QEFO-INEK-ML method is verified by comparing with some existing DOA estimation methods in several scenarios. Finally, the conclusions of the paper and the follow-up research interests are presented in Section 6.

2. DOA estimation model in impulse noise

Assume a uniformly linear array with M antennas, and N far field narrow-band point source signals incident from $\theta_i (i = 1,2,\cdots,N)$, the wavelength is λ, and the element spacing is d. The lth snapshot data received by the array can be described as

$$\boldsymbol{y}(l) = \boldsymbol{A}(\boldsymbol{\theta})\boldsymbol{s}(l) + \boldsymbol{n}(l) \tag{1}$$

where $\boldsymbol{s}(l)= [s_1(l), s_2(l),\cdots, s_N(l)]^{\mathrm{T}}$ is an $N\times 1$ source vector, $\boldsymbol{y}(l)= [y_1(l), y_2(l),\cdots, y_M(l)]^{\mathrm{T}}$ is an $M\times 1$ array snapshot data vector, $\boldsymbol{n}(l)$ is an $M\times 1$ complex impulse noise vector, which is modeled standard by SαS distribution with the characteristic exponent α, $\boldsymbol{A}(\boldsymbol{\theta})= [\boldsymbol{a}(\theta_1), \boldsymbol{a}(\theta_2),\cdots, \boldsymbol{a}(\theta_N)]$ is an $M\times N$ steering matrix, and the steering vector is $\boldsymbol{a}(\theta_i)= [1, \mathrm{e}^{-\mathrm{j}2\pi d\sin\theta_i/\lambda},\cdots, \mathrm{e}^{-\mathrm{j}2\pi(M-1)d\sin\theta_i/\lambda}]^{\mathrm{T}}$, $\boldsymbol{\theta} = [\theta_1, \theta_2,\cdots, \theta_N]$ is an angel vector of signal source, $i = 1,2,\cdots,N$.

Theoretical analysis demonstrates that the infinite norm exponential kernel covariance matrix for $\boldsymbol{z}(l) = [z_1(l), z_2(l),\cdots, z_M(l)]^{\mathrm{T}}$ can be represented by $\boldsymbol{R}=\begin{bmatrix} R_{11} & R_{12} & \cdots & R_{1M} \\ R_{21} & R_{22} & \cdots & R_{2M} \\ \vdots & \vdots & \ddots & \vdots \\ R_{M1} & R_{M2} & \cdots & R_{MM} \end{bmatrix}$ at the limited snapshot numbers, and the specific representation of $\boldsymbol{R}$ is described as

$$R_{ij} = \frac{1}{L}\sum_{l=1}^{L} z_i(l) z_j^*(l) \exp\left(-\eta|z_i(l) - \mu z_j^*(l)|\right) \tag{2}$$

$$\boldsymbol{z}(l) = \frac{\boldsymbol{y}(l)}{\max\{|y_1(l)|, |y_2(l)|,\cdots, |y_M(l)|\}} \tag{3}$$

where $z_i(l)$ and $z_j(l)$ represent the ith and the jth component of vector $\boldsymbol{z}(l)$, respectively, L denotes the maximum number of snapshots, η denotes the EK size which belongs to [0,1], and μ is a positive constant which belongs to [0,2], $i = 1,2,\cdots,M$, $j = 1,2,\cdots,M$.

According to the ML algorithm, the estimation value of $\boldsymbol{\theta}$ can be obtained via the following function:

$$\hat{\boldsymbol{\theta}} = \arg\max_{\boldsymbol{\theta}} \mathrm{tr}(\boldsymbol{P}_{\boldsymbol{A}}(\boldsymbol{\theta})\boldsymbol{R}) \tag{4}$$

where

$$\boldsymbol{P}_{\boldsymbol{A}}(\boldsymbol{\theta}) = \boldsymbol{A}(\boldsymbol{\theta})(\boldsymbol{A}^{\mathrm{H}}(\boldsymbol{\theta})\boldsymbol{A}(\boldsymbol{\theta}))^{-1}\boldsymbol{A}^{\mathrm{H}}(\boldsymbol{\theta}).$$

In this case, the infinite norm exponential kernel covariance matrix can be used to obtain the estimation value of $\boldsymbol{\theta}$ according to ML algorithm in the impulse noise. The proposed ML DOA estimation method based on infinite norm exponential kernel can be shorted for the INEK-ML method, and which can be used in Gaussian noise (α = 2), the Cauchy noise (α=1), the weak impulse noise ($1 < \alpha < 2$), and the strong impulse noise ($0 < \alpha < 1$).

Beyond that, the proposed INEK-ML method can be not only applicable for uniform linear array (ULA), but also applicable for circular array, planar array and other more complex array structures. The proposed INEK-ML method has a wide range of applications in case of DOA estimation.

3. DOA estimation method based on QEFO algorithm

3.1 QEFO algorithm

Electromagnetic field optimization (EFO) [30] is an optimization algorithm based on the principle of the electromagnetic field in physics, and it is different from the swarm intelligence optimization algorithm which is widely proposed from the biological point. In EFO, due to the effect of the attraction and repulsion of electromagnetic particles in the electromagnetic field, electromagnetic particles keep moving away from the worst solution and towards the best solution. The electrified iron core produces magnetic field and forms electromagnets. The electromagnet has one polarity and it changes with the direction of the current. Electromagnets have two characteristics: attraction and repulsion. The same polarity electromagnets repel each other, while the different polarity electromagnets attract each other. In the EFO algorithm, the strength of attraction is 5%−10% higher than that of repulsion, and the ratio of attraction to repulsion is a golden section ratio, which can promote electromagnetic particles to fully explore the search space of the problem and find an approximate optimal solution [30]. EFO performs well in dealing with general low-dimensional or high-dimensional problems. However, the performance of EFO deteriorates seriously or even fails in dealing with multi-dimensional problems. The EFO algorithm cannot overcome the shortcoming of easily trapping in local optimum, which leads to that the EFO algorithm cannot converge to the optimal solution in dealing with the complex continuous optimization problem.

In view of the theory of the EFO algorithm and quantum computation, a QEFO algorithm is proposed. In QEFO, evolution equations are designed to improve the global search ability. In QEFO, each electromagnetic particle is composed of a group of electromagnets, each

electromagnetic particle represents a point in search space, and a certain number of electromagnetic particles constitute an electromagnetic field. The dimension of the point corresponds to the number of electromagnets contained in the electromagnetic particles. The algorithm stipulates that each electromagnet of electromagnetic particles has the same polarity, that is, the polarity of the electromagnetic particle is the same as that of the electromagnet it contains.

There is an electromagnetic field with K electromagnetic particles, each of the electromagnetic particle possesses its own position. The kth electromagnetic particle's position at the tth iteration is defined as $\hat{\boldsymbol{x}}_k^t = [\hat{x}_{k,1}^t, \hat{x}_{k,2}^t, \cdots, \hat{x}_{k,Q}^t]$ $(k = 1,2,\cdots,K)$, which is mapped by the quantum position $\boldsymbol{x}_k^t = [x_{k,1}^t, x_{k,2}^t, \cdots, x_{k,Q}^t]$, where $0 \leqslant x_{k,q}^t \leqslant 1$ $(q = 1,2,\cdots,Q)$. The specific mapping method is defined as

$$\hat{x}_{k,q}^t = \hat{x}_q^{\text{low}} + x_{k,q}^t(\hat{x}_q^{\text{high}} - \hat{x}_q^{\text{low}}) \tag{5}$$

where $\hat{x}_{k,q}^t \in \left[\hat{x}_q^{\text{low}}, \hat{x}_q^{\text{high}}\right]$, $\hat{x}_q^{\text{low}}$ denotes the lower bound of the qth electromagnet, and $\hat{x}_q^{\text{high}}$ denotes the upper bound of the qth electromagnet.

The position of each electromagnetic particle represents a potential solution for the problem to be solved with Q-electromagnet. Hence, the performance of the potential solution $\hat{\boldsymbol{x}}_k^t$ can be evaluated by calculating the fitness value of electromagnetic particle $\hat{\boldsymbol{x}}_k^t$ according to the fitness function $F(\hat{\boldsymbol{x}}_k^t)$.

According to the feature of QEFO, the region of electromagnetic field is divided into positive field, negative field and neutral field. Electromagnetic particles in QEFO are divided into three categories according to their fitness values: positive polarity electromagnetic particles with larger fitness values, negative polarity electromagnetic particles and neutral electromagnetic particles with middle fitness values, the neutral polarity electromagnetic particles are considered as negative which are almost close to zero. All electromagnetic particles are situated in the corresponding electromagnetic field region. The proposed QEFO adopts two different forms of quantum position updating tactics. The updating equations of the first strategy are presented as follows:

If $\delta_{k,q} < \rho$, the quantum position updating equations are defined as follows:

$$v_{k,q}^{t+1} = r_1(x_{\beta,q}^t - x_{k,q}^t) + r_2(p_{k,q}^t - x_{k,q}^t) \tag{6}$$

$$x_{k,q}^{t+1} = \left| x_{k,q}^t \cdot \cos v_{k,q}^{t+1} + \sqrt{1 - (x_{k,q}^t)^2} \cdot \sin v_{k,q}^{t+1} \right| \tag{7}$$

else

$$v_{k,q}^{t+1} = r_3(g_q^t - x_{k,q}^t) + \varphi r_4(x_{\beta,q}^t - x_{\vartheta,q}^t) - r_5(x_{\zeta,q}^t - x_{\vartheta,q}^t) \tag{8}$$

$$x_{k,q}^{t+1} = \left| x_{k,q}^t \cdot \cos v_{k,q}^{t+1} + \sqrt{1 - (x_{k,q}^t)^2} \cdot \sin v_{k,q}^{t+1} \right| \tag{9}$$

where $\delta_{k,q}$ is a uniform random number in [0,1], ρ is a constant number in [0,1], $\boldsymbol{v}_k^{t+1} = [v_{k,1}^{t+1}, v_{k,2}^{t+1}, \cdots, v_{k,Q}^{t+1}]$ denotes the quantum rotations angle, $\varphi = (\sqrt{5}+1)/2$ is the golden ratio, r_1, r_2, r_3, r_4 and r_5 are the uniform random numbers in [0,1], β, ϑ and ζ represent the quantum position labels of electromagnetic particles which are randomly selected in positive field, neutral field and negative field, respectively, $x_{k,q}^t$ represents the qth dimension of the quantum position $\boldsymbol{x}_k^t = [x_{k,1}^t, x_{k,2}^t, \cdots, x_{k,Q}^t]$, $p_{k,q}^t$ represents the qth dimension of the local optimal quantum position $\boldsymbol{p}_k^t = [p_{k,1}^t, p_{k,2}^t, \cdots, p_{k,Q}^t]$ which is searched by the kth electromagnetic particle at the tth iteration, g_q^t represents the qth dimension of the global optimal quantum position $\boldsymbol{g}^t = [g_1^t, g_2^t, \cdots, g_Q^t]$ which is searched by all electromagnetic particles until the tth iteration, $q = 1,2,\cdots,Q$.

In the second strategy of electromagnetic particle's quantum position updating, the quantum position is updated by changing the search size and direction, which is described as

$$v_{k,q}^{t+1} = u_1(b_q^t - x_{k,q}^t) + u_2(g_q^t - x_{k,q}^t) \tag{10}$$

$$x_{k,q}^{t+1} = \left| x_{k,q}^t \cdot \cos v_{k,q}^{t+1} + \sqrt{1 - (x_{k,q}^t)^2} \cdot \sin v_{k,q}^{t+1} \right| \tag{11}$$

where u_1 and u_2 represent random numbers which obey the Gaussian distribution with the mean 0 and the variance 1, and $b_q^t = (1/K)\sum_{k=1}^{K} p_{k,q}^t$ denotes the qth dimension of the average value of K local optimal quantum positions, $\boldsymbol{b}^t = [b_1^t, b_2^t, \cdots, b_Q^t]$.

3.2 Computational complexity analysis of QEFO

In QEFO, the population size is K, the quantum coding length is Q which represents the dimension of the optimization problem, the computational complexity of the QEFO algorithm at each iteration can be calculated as follows: the computational complexity of updating quantum rotation angles is $O(KQ)$, the computational complexity of updating quantum positions is $O(2KQ)$, the computational complexity of calculating the fitness value of the updated positions is $O(K)$, the computational complexity of updating the global optimal quantum position by means of the greedy selection is $O(K)$, and the computational complexity of updating the positive field, neutral field and negative field is $O(K)$. According to the operation rule of symbol O, the total computational complexity of the QEFO algorithm is $O(t_{\max}(3KQ+3K))$ when the maximum number of iterations $t_{\max}$ is reached.

3.3 QEFO-INEK-ML method for DOA estimation

In QEFO, all dimensions of the initial electromagnetic particle's quantum position are randomly generated in [0,1]. For the proposed QEFO-INEK-ML method, the fitness function is defined as

$$F(\hat{\boldsymbol{x}}_k^t) = \mathrm{tr}(\boldsymbol{P}_A(\hat{\boldsymbol{x}}_k^t)\boldsymbol{R}) \tag{12}$$

where the position of the electromagnetic particle $\hat{\boldsymbol{x}}_k^t = [\hat{x}_{k,1}^t, \hat{x}_{k,2}^t, \cdots, \hat{x}_{k,Q}^t]$ can be considered as the estimation values of angles, $Q = N$, and N represents the number of targets.

As the above description, the DOA estimation problem to be solved in this paper can be considered as a continuous problem, and two updating strategies of the quantum position are adopted in the processing of QEFO until the maximum number of iterations has been attained. The QEFO-INEK-ML method for DOA estimation is presented in Algorithm 1.

Algorithm 1 The QEFO-INEK-ML method for DOA estimation

1 **Input**: system parameters of DOA estimation;

2 **Initialize** parameter settings and the initial population of QEFO;

3 $t = 1$ // the first iteration;

4 Randomly generate the initial quantum positions of K electromagnetic particles in [0,1], and mapping them to the corresponding positions of K electromagnetic particles;

5 Calculate the fitness values of the initial positions of all electromagnetic particles according to the fitness function (12), in the light of the fitness values, select the global optimal;

6 Select the global optimal quantum position $\boldsymbol{g}^t$;

7 **while** $t \leqslant t_{\max}$

8 Update the present quantum positions of electromagnetic particles using two strategies, and the probability of each strategy being selected is 50%;

9 **if** $\rho < 0.5$(the first strategies)

10 Update the quantum position by (6) and (7);

11 **else**

12 Update the quantum position by (8) and (9);

13 **end if**

14 Update the quantum position by (10) and (11);

15 Map each quantum position and calculate the fitness;

16 In the light of the new fitness values, select the global optimal quantum position by greedy selection, and divide the electromagnetic particles into positive field, neutral field and negative field;

17 Let $t = t + 1$;

18 **end while**

19 Obtain the optimal estimation values of angles after $t_{\max}$ iterations;

20 **Output:** the optimal DOA estimation results.

3.4 Convergence analysis of QEFO algorithm

Definition 1 The population size of QEFO is K, $\hat{\boldsymbol{X}}$ is the search space of electromagnetic particles, which contains all possible solutions, $\hat{\boldsymbol{X}}^t = \{\hat{\boldsymbol{x}}_1^t, \hat{\boldsymbol{x}}_2^t, \cdots, \hat{\boldsymbol{x}}_K^t, \hat{\boldsymbol{g}}^t\}$ represents the set of positions and the global optimal position at the tth iteration, and F is the fitness function of $\hat{\boldsymbol{X}}$. The $\boldsymbol{\varepsilon}$ acceptable domain of the QEFO is described as

$$\boldsymbol{R}_\varepsilon = \{\hat{\boldsymbol{g}}^t \in \hat{\boldsymbol{X}}^t | F(\hat{\boldsymbol{g}}^t) > \hat{\varphi} + \varepsilon\} \tag{13}$$

where $\varepsilon > 0$, and if QEFO finds a position in $\boldsymbol{R}_\varepsilon$, it is assumed that QEFO finds an acceptable position with an error of ε.

Definition 2 The global convergence of the QEFO algorithm means that sequence $\{F(\hat{\boldsymbol{g}}^t)\}_{t=1}^{\infty}$ should converge to the supremum of fitness function F on $\hat{\boldsymbol{X}}$, the supremum $\hat{\varphi}$ is defined as

$$\hat{\varphi} = \sup(\gamma : \mathrm{vol}[\hat{\boldsymbol{g}}^t \in \hat{\boldsymbol{X}}^t | F(\hat{\boldsymbol{g}}^t) > \gamma] > 0) \tag{14}$$

where vol[$\boldsymbol{C}$] represents the Lebesgue measure on the set of $\boldsymbol{C}$, and $\boldsymbol{C} \in \hat{\boldsymbol{X}}$.

Lemma 1 In QEFO algorithm, hypothesis $F(\hat{\boldsymbol{g}}^{t+1}) \geqslant F(\hat{\boldsymbol{g}}^t)$, and if $\hat{\boldsymbol{x}}^t \in \hat{\boldsymbol{X}}^t$, then $F(\hat{\boldsymbol{g}}^{t+1}) \geqslant F(\hat{\boldsymbol{x}}^t)$.

Proof The conclusion is obvious, because the QEFO algorithm uses the optimal solution retention strategy. With the increase of iterations, the value of the optimal objective function in the electromagnetic field is non-decreasing. □

Lemma 2 $\hat{\boldsymbol{C}}$ is an any Borel subset of $\hat{\boldsymbol{X}}$, if vol[$\hat{\boldsymbol{C}}$] > 0, then $\prod_{t=0}^{\infty}(1 - \ell_t[\hat{\boldsymbol{C}}]) = 0$, where $\ell_t[\hat{\boldsymbol{C}}]$ is the probability of measure ℓ_t arriving at $\hat{\boldsymbol{C}}$.

Proof There are three ways to generate electromagnetic particles which can increase the diversity of population in the progress of QEFO, and that can be described by (6) to (7), (8) to (9) and (10) to (11), respectively. The evolution of the optimal solution is accomplished by updating the quantum position, and the quantum position can be linearly mapped to the position. □

Condition 1 All dimensions of the electromagnetic particle's position are distributed independently, on the basis of (6) and (8) which can generate quantum rotation, all dimensions of the electromagnetic particle's position follows uniform random distribution, and the kth position's probability density function (PDF) is described as

$$f_u(\hat{\boldsymbol{x}}_k^t)=\begin{cases}\dfrac{1}{\prod\limits_{q=1}^{Q}(\hat{x}_q^{\text{high}}-\hat{x}_q^{\text{low}})}, & \hat{\boldsymbol{x}}_k^t\in\hat{\boldsymbol{X}}\\ 0, & \text{else}\end{cases}. \tag{15}$$

Therefore, for any Borel subset $\hat{\boldsymbol{C}}$ which belongs to $\hat{\boldsymbol{X}}$, there is

$$\ell_k^t[\hat{\boldsymbol{C}}]=\int_{\hat{\boldsymbol{C}}} f_u(\hat{\boldsymbol{x}}_k^t)\mathrm{d}\hat{x}_{k,1}^t\mathrm{d}\hat{x}_{k,2}^t,\cdots,\mathrm{d}\hat{x}_{k,Q}^t. \tag{16}$$

For all t, there is

$$E(\hat{x}_{k,q})<\infty. \tag{17}$$

Thus, there must be

$$0<\ell_k^t[\hat{\boldsymbol{C}}]<1 \tag{18}$$

$$\boldsymbol{K}_k^t=\boldsymbol{R}^N\supset\hat{\boldsymbol{X}} \tag{19}$$

where $\boldsymbol{K}_k^t$ is the support of ℓ_k^t in $\hat{\boldsymbol{X}}$, and $\hat{\boldsymbol{C}}\supset\boldsymbol{K}_k^t$. Then, we can get

$$\boldsymbol{K}^t=\bigcup_{k=1}^{K}\boldsymbol{K}_k^t=\boldsymbol{R}^N\supset\hat{\boldsymbol{X}} \tag{20}$$

where $\boldsymbol{K}^t$ is the support of ℓ^t. The probability measure on $\hat{\boldsymbol{C}}$ generated by ℓ^t can be calculated as

$$\ell^t[\hat{\boldsymbol{C}}]=1-\prod_{k=1}^{K}(1-\ell_k^t[\hat{\boldsymbol{C}}]). \tag{21}$$

By (18), we can get

$$0<\ell^t[\hat{\boldsymbol{C}}]<1,\quad t=1,2,\cdots \tag{22}$$

$$\prod_{t=1}^{\infty}(1-\ell^t[\hat{\boldsymbol{C}}])=0. \tag{23}$$

Condition 2 All dimensions of the electromagnetic particle's position are distributed independently, on the basis of (10) which can generate quantum rotation, all dimensions of the electromagnetic particle's position follows Gaussian distribution, and the kth position's PDF is described as

$$f_g(\hat{\boldsymbol{x}}_k^t)=\left(\frac{1}{2\pi}\right)^{Q}\prod_{q=1}^{Q}\exp\left(\frac{-(\hat{x}_{k,q}^t-\hat{x}_q^{\text{low}})^2}{2(\hat{x}_q^{\text{high}}-\hat{x}_q^{\text{low}})^2}\right). \tag{24}$$

In this case, we can obtain the same conclusion as Condition 1, and the proof process resembles Condition 1.

Theorem 1 QEFO is a global convergent algorithm.

Proof According to Lemma 1, if $\hat{\boldsymbol{x}}_b^t\in\boldsymbol{R}_\varepsilon$ or $\varepsilon^t\in\boldsymbol{R}_\varepsilon$, for $\forall t^+>t$, there is, $\hat{\boldsymbol{x}}_b^{t^+}\in\boldsymbol{R}_\varepsilon$, from this we can get

$$P[\hat{\boldsymbol{x}}^t\in\boldsymbol{R}_\varepsilon]=1-P[\hat{\boldsymbol{x}}^t\in\hat{\boldsymbol{X}}|\boldsymbol{R}_\varepsilon]\geqslant 1-\prod_{\tau=1}^{t}(1-\ell^\tau[\boldsymbol{R}_\varepsilon]) \tag{25}$$

where $P[\hat{\boldsymbol{x}}^t\in\boldsymbol{R}_\varepsilon]$ represents probability of $\hat{\boldsymbol{x}}^t\in\boldsymbol{R}_\varepsilon$ and $\hat{\boldsymbol{X}}|\boldsymbol{R}_\varepsilon$ denotes the domain in $\hat{\boldsymbol{X}}$ where $\boldsymbol{R}_\varepsilon$ is removed. Taking limit and considering ℓ^t as probability measure, we can get

$$1\geqslant\lim_{t\to+\infty}P[\hat{\boldsymbol{x}}^t\in\boldsymbol{R}_\varepsilon]\geqslant 1-\lim_{t\to+\infty}\prod_{\tau=1}^{t-1}(1-\ell^\tau[\boldsymbol{R}_\varepsilon]). \tag{26}$$

According to Lemma 2, we can get

$$1\geqslant\lim_{t\to+\infty}P[\hat{\boldsymbol{x}}^t\in\boldsymbol{R}_\varepsilon]\geqslant 1-0 \tag{27}$$

$$\lim_{t\to+\infty}P[\hat{\boldsymbol{x}}^t\in\boldsymbol{R}_\varepsilon]=1. \tag{28}$$

The above process shows that QEFO can converge to the global optimal solution. □

4. Performance analysis for DOA estimation in the impulse noise

4.1 Basic definitions in the impulse noise model

In practical environments, the scattering intensity of the target obeys the Gaussian distribution. However, the noise is impulse noise with the heavy tail in the PDF. In the DOA estimation model which is given by Section 2, it is assumed that the noise among the elements of the receiving array is a zero-mean independent and identically distributed SαS process, and the characteristic function SαS distribution is described as

$$\phi(w)=\mathrm{e}^{-\gamma^\alpha|w|^\alpha} \tag{29}$$

where $0<\alpha\leqslant 2$ represents the characteristic exponent, $\gamma>0$ represents the scale, and γ^2 is similar to the variance of Gaussian distribution.

The tail of the PDF for SαS distribution can be described by the characteristic exponent α[31]. Because the second and higher order moment of SαS distribution are not existing, the SNR for SαS distribution is normally notable. Based on the above description, the GSNR can be defined as

$$\text{GSNR}=10\lg\left\{\frac{\mathrm{E}[\|\boldsymbol{s}(l)\|^2]}{\gamma^\alpha}\right\} \tag{30}$$

where $\mathrm{E}[\|\boldsymbol{s}(l)\|^2]$ denotes the average power of the signals.

4.2 CRB in the impulse noise

CRB is proposed for parameter (or parameters) estimation, which determines a lower limit for the variance (or covariance matrix) of any unbiased estimator. It is impossible to obtain unbiased estimators whose variances are less than CRB, and CRB provides a criterion for comparing the performance of unbiased estimators. The vari-

ance of unbiased estimators can only approximate CRB without restriction, but not less than CRB.

$$\boldsymbol{y}(l)=\boldsymbol{A}(\boldsymbol{\theta})\boldsymbol{s}(l)+\boldsymbol{n}(l)=\Im(\boldsymbol{\chi},l)+\boldsymbol{h}(l) \tag{31}$$

where $\Im(\boldsymbol{\chi},l)$ and $\boldsymbol{h}(l)$ denote the signal component and the noise component at the l th snapshot, respectively, $\boldsymbol{\chi}=[\boldsymbol{\theta},\bar{\boldsymbol{s}}(1),\bar{\boldsymbol{s}}(2),\cdots,\bar{\boldsymbol{s}}(L),\tilde{\boldsymbol{s}}(1),\tilde{\boldsymbol{s}}(2),\cdots,\tilde{\boldsymbol{s}}(L)]$, $\boldsymbol{h}(l)=[h_1(l),h_2(l),\cdots,h_M(l)]^{\mathrm{T}}$, $h_m(l)=\bar{h}_m(l)+\tilde{h}_m(l)$, $m=1,2,\cdots,M$. We define $\{\bar{\cdot}\}$ is the real part of $\{\cdot\}$ and $\{\tilde{\cdot}\}$ is the imaginary part of $\{\cdot\}$.

In general, the CRB matrix of $\boldsymbol{\chi}$ is defined as the inverse Fisher information matrix (FIM) $\boldsymbol{J}$:

$$\mathrm{CRB}(\hat{\boldsymbol{\chi}})\geqslant\boldsymbol{J}^{-1} \tag{32}$$

where $\hat{\boldsymbol{\chi}}$ is an estimate of $\boldsymbol{\chi}$, and the element of $\boldsymbol{J}$ is given by

$$J_{ij}=\mathrm{E}\left[\frac{\partial\ln f(\boldsymbol{Y}/\boldsymbol{\chi})}{\partial\chi_i}\frac{\partial\ln f(\boldsymbol{Y}/\boldsymbol{\chi})}{\partial\chi_j}\right] \tag{33}$$

where $\boldsymbol{Y}=[\boldsymbol{y}(1),\boldsymbol{y}(2),\cdots,\boldsymbol{y}(L)]$, $f(\boldsymbol{Y}/\boldsymbol{\chi})$ is the PDF of $\boldsymbol{Y}$ which can be represented as

$$f(\boldsymbol{Y}/\boldsymbol{\chi})=\prod_{l=1}^{K}\prod_{m=1}^{M}f_h[\bar{h}_m(l),\tilde{h}_m(l)] \tag{34}$$

where $\bar{h}_m(l)=\bar{y}_m(l)-\bar{\Im}_m(\boldsymbol{\chi},l)$, $\tilde{h}_m(l)=\tilde{y}_m(l)-\tilde{\Im}_m(\boldsymbol{\chi},l)$, and $f_h(\bar{h},\tilde{h})$ represents the PDF with parameter $\boldsymbol{\Omega}$ that satisfies the condition of regularity [32], then the element of $\boldsymbol{J}$ can be expressed as

$$\begin{aligned}J_{ij}=I_{\mathrm{r}}(\boldsymbol{\Omega})\sum_{l=1}^{L}\sum_{m=1}^{M}\frac{\partial\bar{\Im}_m(\boldsymbol{\chi},l)}{\partial\chi_i}\frac{\partial\bar{\Im}_m(\boldsymbol{\chi},l)}{\partial\chi_j}+\\ I_{\mathrm{i}}(\boldsymbol{\Omega})\sum_{l=1}^{L}\sum_{m=1}^{M}\frac{\partial\tilde{\Im}_m(\boldsymbol{\chi},l)}{\partial\chi_i}\frac{\partial\tilde{\Im}_m(\boldsymbol{\chi},l)}{\partial\chi_j}\end{aligned} \tag{35}$$

where the real part and the imaginary part of scaling factor can be described as follows:

$$I_{\mathrm{r}}(\boldsymbol{\Omega})=\mathrm{E}\left\{\left[\frac{\frac{\partial}{\partial\bar{h}}f_h(\bar{h},\tilde{h})}{f_h(\bar{h},\tilde{h})}\right]^2\right\}, \tag{36}$$

$$I_{\mathrm{i}}(\boldsymbol{\Omega})=\mathrm{E}\left\{\left[\frac{\frac{\partial}{\partial\tilde{h}}f_h(\bar{h},\tilde{h})}{f_h(\bar{h},\tilde{h})}\right]^2\right\}. \tag{37}$$

Suppose $f_h(\bar{h},\tilde{h})$ is circularly symmetric, and then $f_h(\pm\bar{h},\pm\tilde{h})=f_h(\bar{h},\tilde{h})=f_h(\sqrt{\bar{h}^2+\tilde{h}^2})$ which means $\bar{h}_m(k)$ and $\tilde{h}_m(k)$ are uncorrelated with zero-mean. Hence, we can gain that $I_{\mathrm{r}}(\boldsymbol{\Omega})$ and $I_{\mathrm{i}}(\boldsymbol{\Omega})$ are equivalent to the caling factor $I_{\mathrm{c}}(\boldsymbol{\Omega})$, and $I_{\mathrm{c}}(\boldsymbol{\Omega})$ can be denoted as

$$I_{\mathrm{c}}(\boldsymbol{\Omega})=\pi\int_0^{\infty}\frac{[f'(\wp)]^2}{f(\wp)}\wp\mathrm{d}\wp. \tag{38}$$

We have

$$\boldsymbol{J}=\begin{bmatrix}\hat{w}&0&\cdots&0&0\\ \boldsymbol{0}&\boldsymbol{G}&\cdots&\boldsymbol{0}&\boldsymbol{\Delta}_1\\ \vdots&\vdots&\ddots&\vdots&\vdots\\ \boldsymbol{0}&\boldsymbol{0}&\cdots&\boldsymbol{G}&\boldsymbol{\Delta}_L\\ \boldsymbol{0}&\boldsymbol{\Delta}_1^{\mathrm{T}}&\cdots&\boldsymbol{\Delta}_L^{\mathrm{T}}&\boldsymbol{\Gamma}\end{bmatrix}, \tag{39}$$

$$\boldsymbol{J}^{-1}=\left(\boldsymbol{\Gamma}-\sum_{l=1}^{L}\boldsymbol{\Delta}_l^{\mathrm{T}}\boldsymbol{G}^{-1}\boldsymbol{\Delta}_l\right)^{-1}, \tag{40}$$

where

$$\boldsymbol{G}=\begin{bmatrix}\bar{\boldsymbol{H}}&-\tilde{\boldsymbol{H}}\\ \tilde{\boldsymbol{H}}&\bar{\boldsymbol{H}}\end{bmatrix}$$

$$\boldsymbol{H}=I_{\mathrm{c}}(\boldsymbol{\Omega})\boldsymbol{A}(\boldsymbol{\theta})^{\mathrm{H}}\boldsymbol{A}(\boldsymbol{\theta})$$

$$\boldsymbol{\Delta}_l=\left[\bar{\boldsymbol{\Delta}}(l),\tilde{\boldsymbol{\Delta}}(l)\right]^{\mathrm{H}}$$

$$\boldsymbol{\Delta}(l)=I_{\mathrm{c}}(\boldsymbol{\Omega})\boldsymbol{A}(\boldsymbol{\theta})^{\mathrm{H}}\boldsymbol{D}\boldsymbol{S}(l)$$

$$\boldsymbol{\Gamma}=I_{\mathrm{c}}(\boldsymbol{\Omega})\sum_{l=1}^{L}\mathrm{Re}\left\{\boldsymbol{S}(l)^{\mathrm{H}}\boldsymbol{D}^{\mathrm{H}}\boldsymbol{D}\boldsymbol{S}(l)\right\}$$

$$\boldsymbol{D}=[\boldsymbol{d}(\theta_1),\boldsymbol{d}(\theta_2),\cdots,\boldsymbol{d}(\theta_N)]$$

$$\boldsymbol{d}(\theta_n)=\partial\boldsymbol{a}(\theta_n)/\partial\theta_n$$

$$\boldsymbol{S}(l)=\mathrm{diag}\{s_1(l),s_2(l),\cdots,s_N(l)\}.$$

According to the above analysis, the CRB can be calculated as

$$\mathrm{CRB}(\boldsymbol{\theta})=\left(I_{\mathrm{c}}(\boldsymbol{\Omega})\sum_{l=1}^{L}\mathrm{Re}\left\{\boldsymbol{s}(l)^{\mathrm{H}}\boldsymbol{D}^{\mathrm{H}}\boldsymbol{P}_{\boldsymbol{A}}^{\perp}\boldsymbol{D}\boldsymbol{s}(l)\right\}\right)^{-1} \tag{41}$$

where $\boldsymbol{P}_{\boldsymbol{A}}^{\perp}=\boldsymbol{I}-\boldsymbol{P}_{\boldsymbol{A}}$, $\boldsymbol{P}_{\boldsymbol{A}}=\boldsymbol{A}(\boldsymbol{\theta})\left(\boldsymbol{A}(\boldsymbol{\theta})^{\mathrm{H}}\boldsymbol{A}(\boldsymbol{\theta})\right)^{-1}\boldsymbol{A}(\boldsymbol{\theta})^{\mathrm{H}}$ and $\boldsymbol{P}_{\boldsymbol{A}}^{\perp}$ denotes projection onto the orthogonal complementary space of $\boldsymbol{A}(\boldsymbol{\theta})$.

It is obvious from (41) that the CRB for the DOA is composed by the product of two parts, which depends on the PDF of impulse noise and the signal, respectively. The effect of impulse noise on CRB is realized by $I_{\mathrm{c}}(\boldsymbol{\Omega})$. Because the PDF of impulse noise has no closed-form expression, except for α=1 and α= 2 (Cauchy and Gaussian distribution, respectively), it is a difficult problem to obtain the CRB for angle estimation [33].

Based on this background, an approximate model for SαS PDF is adopted in this paper, which is bi-parameter Cauchy Gaussian mixture model (BCGM) [34]. The SαS PDF is described as

$$f(\wp)=(1-\hat{\varepsilon})f_{\mathrm{G}}(\wp)+\hat{\varepsilon}f_{\mathrm{C}}(\wp)=$$

$$(1-\hat{\varepsilon})\frac{1}{2\gamma\sqrt{\pi}}\exp\left(-\frac{\wp^2}{4\gamma^2}\right)+\hat{\varepsilon}\frac{\gamma}{\pi(\wp^2+\gamma^2)} \tag{42}$$

where $\hat{\varepsilon}$ represents the mixture ratio, and γ denotes the scale exponent of the SαS distribution.

5. Simulation results and discussion

For the sake of assessing the angle estimation performance of QEFO-INEK-ML, a series of experiments are conducted in this section. A uniform linear array with $d=\lambda/2$ is used, η=0.5, μ=0.35. For the QEFO, Q=30, $t_{\max}$=100, P_{field}=0.1, N_{field}=0.4, ρ=0.2. For the purpose of ensuring the reliability of simulation results, the number of Monte-Carlo experiments is set to 600 in all scenarios.

In the next simulation experiments, the performances of QEFO-INEK-ML, IN-MUSIC [18], ROC-MUSIC [15] ($\tilde{\alpha}$=1), FLOM-MUSIC [16] ($\tilde{\alpha}$=1.2), FLOC-MUSIC [17] ($\tilde{\alpha}$=0.6), FLOM [35]-ML [8] ($\tilde{\alpha}$=1.2), and the CRB are compared, where $\tilde{\alpha}$ denotes the fractional order.

5.1 The first scenario

Firstly, two independent sources located at $\theta_1=20°$ and $\theta_2=30°$ are taken into account in this scenario. In order to examine the accuracy of DOA estimation, the root mean square error (RMSE) is defined as

$$\text{RMSE}=\sqrt{\sum_{i=1}^{N}\sum_{\hat{n}=1}^{N_{\text{ex}}}\frac{(\theta_i-\hat{\theta}_i^{\hat{n}})^2}{NN_{\text{ex}}}} \tag{43}$$

where N and N_{ex} represent the number of sources and the number of Monte-Carlo experiments, respectively, θ_i denotes the true angle of DOA for the ith source, and $\hat{\theta}_i^{\hat{n}}$ denotes the estimated angle of DOA for the ith source in the $\hat{n}$th experiment.

In order to assess the performance of QEFO-INEK-ML under the conditions in different numbers of snapshots, the RMSE and CRB simulation comparison curves are plotted in Fig. 1 with M=8, GSNR = 10 dB, α=1.5, $\hat{\varepsilon}$=0.4 and γ=1. The simulation results show that the gap between the RMSE of QEFO-INEK-ML and CRB is the smallest, it means that the angle estimation results obtained by QEFO-INEK-ML about two independent sources in the case of impulse noise are more accurate. Beyond that, the performance of the proposed QEFO-INEK-ML method outperforms five other methods in terms of estimation accuracy under the small number of snapshots.

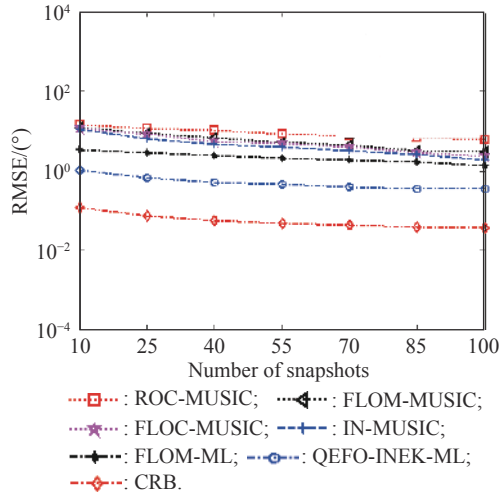

Fig. 1 RMSE and CRB simulation comparison curves in different numbers of snapshots

The angle estimation success rate simulation comparison curves of two independent sources under the conditions in different numbers of snapshots with GSNR= 10 dB and α=1.5 are plotted in Fig. 2, which demonstrates the ability of effective estimation of six DOA estimation methods. When the absolute deviation between the estimated angle and the real angle is no more than 1°, the angle estimation is considered to be successful. It is clearly that the ability of effective target estimation of the QEFO-INEK-ML method in the impulse noise outperforms that of five other methods, especially in the case of small-snapshot domain. The robustness of the QEFO-INEK-ML DOA estimation method is more excellent in the impulse noise.

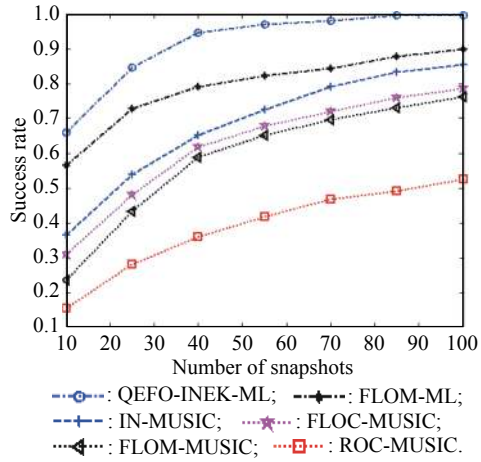

Fig. 2 Success rate simulation comparison curves in different numbers of snapshots

5.2 The second scenario

In previous simulation scenarios, we only consider two sources. Hence, in order to verify whether the different

numbers of sources will affect the estimation performance of the proposed QEFO-INEK-ML method, three independent sources located at θ_1=20°, θ_2=30°, θ_3=40° are used in this scenario, the number of antennas $M=10$, and the setting of other parameters is the same as the second scenario.

As for the number of independent sources is three, the RMSE and CRB simulation comparison curves in different GSNRs with α=1.5 are given in Fig. 3, the relationship between the success rate and GSNR with α=1.5 is presented in Fig. 4, and the relationship between the success rate and the characteristic exponent with GSNR=10 dB is given in Fig. 5. From Fig. 3, Fig. 4 and Fig. 5, a conclusion can be obtained that the proposed QEFO-INEK-ML method has an excellent angle estimation performance. Further more, the other conclusions resemble those obtained in the previous experiments.

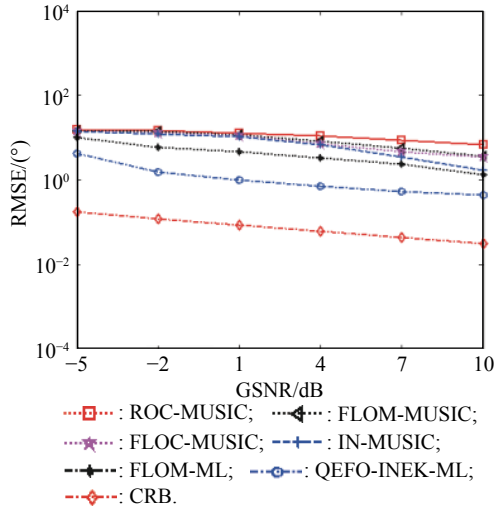

Fig. 3 RMSE and CRB simulation comparison curves for three independent sources in different GSNRs

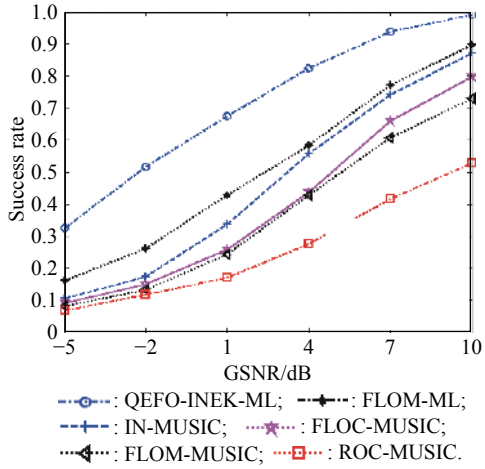

Fig. 4 Success rate simulation comparison curves for three independent sources in different GSNRs

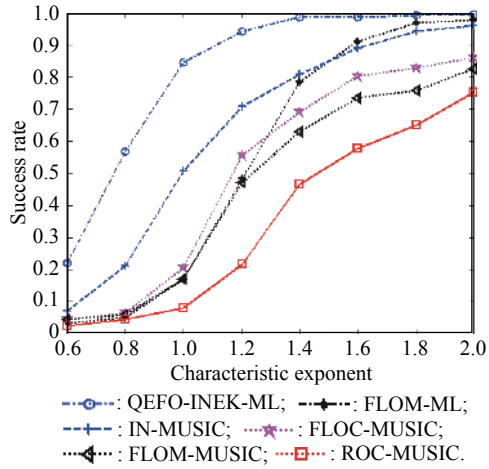

Fig. 5 Success rate simulation comparison curves for three independent sources in different characteristic exponents

5.3 The third scenario

The previous simulation experiments only consider the case of independent sources, and are unable to examine the effectiveness of the proposed QEFO-INEK-ML method for coherent sources. As we all know, it is more difficult to estimate coherent sources, and coherent sources often lead to a serious deterioration in the DOA estimation performance of ROC-MUSIC method, FLOM-MUSIC method, FLOC-MUSIC method and IN-MUSIC method [36]. Therefore, the forward-backward spatial smoothing (SS) method is adopted in this scenario to deal with the coherent sources [37,38].

Two coherent sources located at θ_1= 20° and θ_2= 30° are taken into account to verify the influence of coherent sources on the performance of the proposed QEFO-INEK-ML DOA estimation method. The number of antennas M=8, and the other parameters are the same as the second scenario.

As for two coherent sources, the RMSE and CRB simulation comparison curves in different GSNRs with α=1.5 are given in Fig. 6, the effect of GSNR on the success rate in the case of α=1.5 is presented in Fig. 7, and the effect of the characteristic exponent on the success rate with GSNR=10 dB is given in Fig. 8. From Fig. 6, Fig. 7 and Fig. 8, we can receive a conclusion that the proposed QEFO-INEK-ML method still has an excellent angle estimation performance for coherent sources, and it outperforms five other methods in terms of the estimation accuracy and the success rate. According to the above analysis, it is obvious that the proposed QEFO-INEK-ML method can locate coherent sources without deteriorating performance, which proves the robustness and superiority of the QEFO-INEK-ML method.

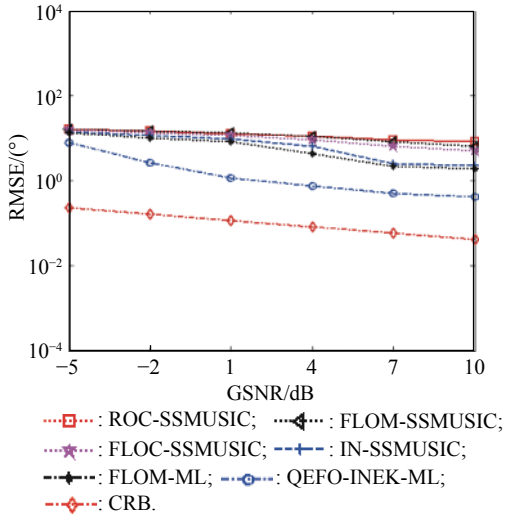

Fig. 6 RMSE and CRB simulation comparison curves for two coherent sources in different GSNRs

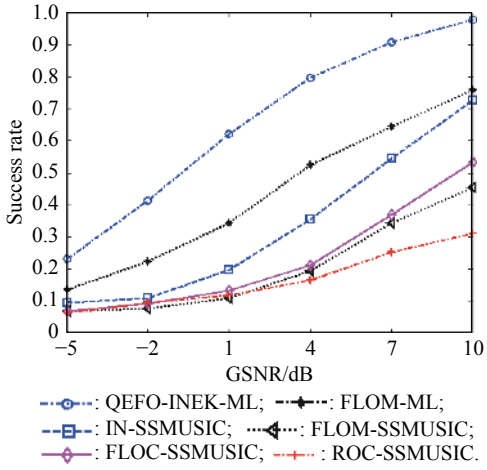

Fig. 7 Success rate simulation comparison curves for two coherent sources in different GSNRs

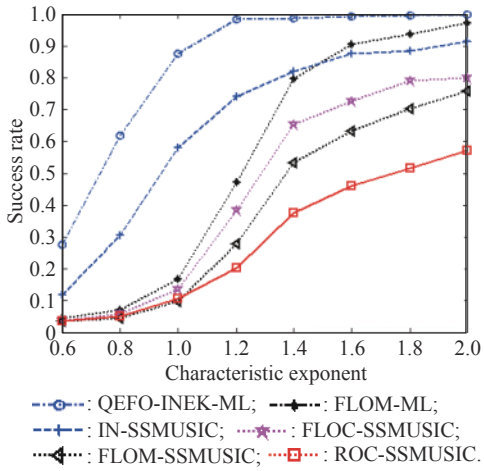

Fig. 8 Success rate simulation comparison curves for two coherent sources in different characteristic exponents

6. Conclusions

We propose a QEFO-INEK-ML DOA estimation method to locate the directions of targets in the impulse noise in this paper. The simulation results show that the proposed QEFO-INEK-ML method can locate independent sources and coherent sources under the complex impulse noise environment, effectively. The proposed QEFO-INEK-ML method can obtain more preeminent performance compared with some previous methods in the case of snapshot deficiency and the strong impulse noise, and it tests the superiority and robustness of the QEFO-INEK-ML method. Beyond that, we prove the convergence of the QEFO algorithm by mathematical analysis, and we obtain the general CRB which can be used for DOA estimation in the impulse noise. In the follow-up study, we will design a multiple objective quantum electromagnetic field optimization algorithm to resolve more complex DOA estimation problems.

References

[1] YAN F G, GONG J J, LIU S, et al. Joint cross covariance matrix based fast direction of arrival estimation. Systems Engineering and Electronics, 2018, 40(4): 733–738. (in Chinese)

[2] TIAN Y, SHI J X, WANG Y R, et al. Non-coherent direction of arrival estimation utilizing linear model approximation. Signal Processing, 2019, 157: 261–265.

[3] LIU Z M, ZHANG C W, YU P S. Direction-of-arrival estimation based on deep neural networks with robustness to array imperfections. IEEE Trans. on Antennas and Propagation, 2018, 66(12): 7315–7326.

[4] SCHMIDT O. Multiple emitter location and signal parameter estimation. IEEE Trans. on Antennas and Propagation, 1986, 34(3): 276–280.

[5] MENG D D, WANG X P, HUANG M X, et al. Robust weighted subspace fitting for DOA estimation via block sparse recovery. IEEE Communications Letters, 2020, 24(3): 563–567.

[6] YAN F G, JIN M, LIU S, et al. Real-valued MUSIC for efficient direction estimation with arbitrary array geometries. IEEE Trans. on Signal Processing, 2014, 62(6): 1548–1560.

[7] ZHANG Y, NG B P. MUSIC-like DOA estimation without estimating the number of source. IEEE Trans. on Signal Processing, 2010, 58(3): 1668–1676.

[8] JAFFER A G. Maximum likelihood direction finding of stochastic sources: a separable solution. Proc. of the International Conference on Acoustics, Speech, and Signal Processing, 1988: 2893−2896.

[9] SWINDLEHURST A, VIBERG M. Subspace fitting with diversely polarized antenna arrays. IEEE Trans. on Antennas and Propagation, 1993, 41(12): 1687–1694.

[10] HAN F M, ZHANG X D. An ESPRIT-like algorithm for coherent DOA estimation. IEEE Antennas and Wireless Propagation Letters, 2005, 4: 443–446.

[11] ROY R, KAILATH T. ESPRIT-estimation of signal parameters via rotational invariance techniques. IEEE Trans. on Acoustics, Speech, and Signal Processing, 1989, 37(7): 984–995.

[12] LIU M Y, GAO H, WU Y T. Improved subspace-based method for 2D DOA estimation with L-shaped array. Elec-

tronics Letters, 2020, 56(8): 402–404.
[13] MA J T, QIU T S. Automatic modulation classification using cyclic correntropy spectrum in impulsive noise. IEEE Wireless Communications Letters, 2019, 8(2): 440–443.
[14] LUO K X, WU M P, FAN Y. Robust adaptive filtering based on maximum entropy method and its application. Systems Engineering and Electronics, 2020, 42(3): 667–673. (in Chinese)
[15] TSAKALIDES P, NIKIAS C L. The robust covariation-based MUSIC (ROC-MUSIC) algorithm for bearing estimation in impulsive noise environments. IEEE Trans. on Signal Processing, 1996, 44(7): 1623–1633.
[16] LIU T H, MENDEL J M. A subspace-based direction finding algorithm using fractional lower order statistics. IEEE Trans. on Signal Processing, 2001, 49(8): 1605–1613.
[17] YOU G H, QIU T S, ZHU Y. A novel extended fractional lower order cyclic MUSIC algorithm in impulsive noise. ICIC Express Letters, 2012, 6(9): 2371–2376.
[18] HE J, LIU Z, WONG K T. Snapshot-instantaneous $\|.\|_{\text{infin}}$ normalization against heavy-tail noise. IEEE Trans. on Aerospace and Electronic Systems, 2008, 44(3): 1221–1227.
[19] TSAKALIDES P. Maximum likelihood localization of sources in noise modeled as a stable process. IEEE Trans. on Signal Processing, 1995, 43(11): 2700–2713.
[20] ZHAO Y Z, GAO H Y, DIAO M, et al. Direction finding of maximum likelihood algorithm using artificial bee colony in the impulsive noise. Proc. of the International Conference on Artificial Intelligence and Computational Intelligence, 2010: 102−105.
[21] LIU W F, POKHAREL P P, PRINCIPE J C. Correntropy: properties and applications in non-Gaussian signal processing. IEEE Trans. on Signal Processing, 2007, 55(11): 5286–5298.
[22] SANTAMARIA I, POKHAREL P P, PRINCIPE J C. Generalized correlation function: definition, properties, and application to blind equalization. IEEE Trans. on Signal Processing, 2006, 54(6): 2187–2197.
[23] KENNEDY J, EBERHART R. Particle swarm optimization. Proc. of the IEEE International Conference on Neural Networks, 1995: 1942−1948.
[24] WANG Z G, WANG D M, BAI B, et al. Direction finding algorithm of correlated interferometer based on genetic algorithm with high degree of stretching. Systems Engineering and Electronics, 2018, 40(1): 39–44. (in Chinese)
[25] DERVIS K, BAHRIYE A. A comparative study of artificial bee colony algorithm. Applied Mathematics and Computation, 2009, 214(1): 108–132.
[26] GUO X, YIN S C, ZHANG Y W, et al. Proportional-integral-derivative controller parameter optimisation based on improved glowworm swarm optimisation algorithm. International Journal of Computing Science and Mathematics, 2020, 11(3): 278–290.
[27] HAN Y, JING Y W, DIMIROVSKI G M. An improved fruit fly algorithm-unscented Kalman filter-echo state network method for time series prediction of the network traffic data with noises. Transactions of the Institute of Measurement and Control, 2020, 42(7): 1281–1293.
[28] ZHENG X, GAO Y J, JING W X, et al. Multidisciplinary integrated design of long-range ballistic missile using PSO algorithm. Journal of Systems Engineering and Electronics, 2020, 31(2): 335–349.
[29] GAO H Y, DU Y N, LI C W. Quantum fireworks algorithm for optimal cooperation mechanism of energy harvesting cognitive radio. Journal of Systems Engineering and Electronics, 2018, 29(1): 18–30.
[30] HOSEIN A, SITI M S, ZAHRA B, et al. Electromagnetic field optimization: a physics-inspired metaheuristic optimization algorithm. Swarm and Evolutionary Computation, 2016, 26: 8–22.
[31] HUANG J Y, WANG Q. CRLB for DOA estimation in Gaussian and non-Gaussian mixed environments. Wireless Personal Communications, 2013, 68(4): 1673–1688.
[32] NOAM Y, MESSER H. Notes on the tightness of the hybrid Cramér–Rao lower bound. IEEE Trans. on Signal Processing, 2009, 57(6): 2074–2084.
[33] GAO H Y, LI J, DIAO M. Direction finding of bistatic MIMO radar based on quantum-inspired grey wolf optimization in the impulse noise. EURASIP Journal on Advances in Signal Processing, 2018, 75: 1–14.
[34] LI X T, SUN J, JIN L W, et al. Bi-parameter CGM model for approximation of α-stable PDF. Electronics Letters, 2008, 44(18): 1096–1098.
[35] SHAO M, NIKIAS C L. Signal processing with fractional lower order moments: stable processes and their applications. Proceedings of the IEEE, 1993, 81(7): 986–1010.
[36] GAO H Y, DIAO M. Quantum swarm intelligence and its application in communication technology. Beijing: Publishing House of Electronics Industry, 2016. (in Chinese)
[37] CHOI Y H. On conditions for the rank restoration in forward/backward spatial smoothing. IEEE Trans. on Signal Processing, 2002, 50(11): 2900–2901.
[38] PILLAI S U, KWON B H. Forward/backward spatial smoothing techniques for coherent signal identification. IEEE Trans. on Acoustics, Speech, and Signal Processing, 1989, 37(1): 8–15.

Biographies

DU Yanan was born in 1992. She received her M.S. degree in communication engineering from Harbin Engineering University, Harbin, Heilongjiang, China, in 2017. She is currently working towards her Ph.D. degree in the College of Information and Communication Engineering at Harbin Engineering University, China. Her current research interests include swarm intelligence and signal processing.
E-mail: wenhuamo@126.com

GAO Hongyuan was born in 1977. He received his M.S. and Ph.D. degrees in communication and information systems from Harbin Engineering University in 2005 and 2010, respectively. He is currently an associate professor in the College of Information and Communication Engineering at Harbin Engineering University. His current research interests include intelligence computing, signal processing of radar and wireless communication system.
E-mail: gaohongyuan@hrbeu.edu.cn

CHEN Menghan was born in 1994. She received her B.S. degree from Harbin Engineering University in 2016. Now she is a doctoral candidate of information and communication engineering. She is currently working towards her Ph.D. degree in the College of Information and Communication Engineering at Harbin Engineering University, China. Her current research interests include intelligence computing and array signal processing.
E-mail: moqunjisuan@163.com